PCCP

High-Accuracy First-Principles-based Rate Coefficients for the Reaction of OH and CH_3OOH

Journal:	*Physical Chemistry Chemical Physics*
Manuscript ID	CP-ART-08-2022-003919.R1
Article Type:	Paper
Date Submitted by the Author:	13-Oct-2022
Complete List of Authors:	Nguyen, Thanh Lam; University of Florida, Chemistry Perera, Ajith; University of Florida, Department of Chemistry Peeters, Jozef; KU Leuven, Department of Chemistry

High-Accuracy First-Principles-based Rate Coefficients for the Reaction of OH and CH_3OOH

Thanh Lam Nguyen,[1] and Ajith Perera,[1]
[1]*Quantum Theory Project, Departments of Chemistry and Physics, University of Florida, Gainesville, FL. 32611, USA.*
Jozef Peeters[2,*]
[2]*Department of Chemistry, University of Leuven, Celestijnenlaan 200F, B-3001 Leuven, Belgium.*

Corresponding authors: jozef.peeters@kuleuven.be; tlam.nguyen@chem.ufl.edu

Submitted to *Phys. Chem. Chem. Phys.* on Aug. 24, 2022; Revised on Oct. 13, 2022.

Abstract

The $^{\bullet}$OH-initiated oxidation of methyl hydroperoxide, which plays an important role in the atmospheric chemistry of methane, was theoretically characterized using high-accuracy composite amHEAT-345(Q) coupled-cluster calculations followed by a two-dimensional *E*,*J* resolved master equation analysis. The reaction is found to proceed through two distinct hydrogen-bonded pre-reactive complexes leading to two product channels, in accord with the experimental observations: (i) $^{\bullet}OH + CH_3OOH \rightarrow CH_3OO^{\bullet} + H_2O$ with a yield of 0.8 ± 0.1, and (ii) $^{\bullet}OH + CH_3OOH \rightarrow HCHO + {}^{\bullet}OH + H_2O$ with a yield of 0.2 ± 0.1. The calculated reaction enthalpies are within 0.2 kcal mol^{-1} of the benchmark ATcT values. Overall thermal rate coefficients obtained from first principles are found to be in the low-pressure limit at atmospheric pressure; the total rate coefficient can be expressed over the T = 200-450 K range as $k(T) = 5.0 \times 10^{-12} \times T^{-0.152} \times exp(287/T)$ cm^3 s^{-1}, strongly supporting the experimental results of Vaghjiani and Ravishankara (*J Phys Chem* 1989**,** *93*, 1948), with which this expression agrees within *ca.* 15%. The current results show that (i) is the principal reaction channel and support the view that, due to its inherently fast transformations, CH_3OOH is an important redistribution species for $HO_x^{\bullet}$ radicals in the Earth's atmosphere.

INTRODUCTION

Methyl hydroperoxide (CH_3OOH), the simplest organic peroxide, is mainly produced by the oxidation of methane in the atmosphere under low NO_x conditions (equations 1-3).[1, 2] CH_3OOH is also a key intermediate product in the photo-oxidation of several non-methane volatile organic compounds (NMVOCs), that can proceed through methyl radicals.[3, 4]

$$CH_4 + {}^{\bullet}OH \rightarrow {}^{\bullet}CH_3 + H_2O \quad (1a)$$

$$CH_4 + O(^1D) \rightarrow CH_3OH^* \rightarrow {}^{\bullet}CH_3 + {}^{\bullet}OH \quad (1b)$$

$$^{\bullet}CH_3 + O_2 \rightarrow CH_3OO^{\bullet} \quad (2)$$

$$CH_3OO^{\bullet} + HO_2^{\bullet} \rightarrow CH_3OOH + O_2 \quad (3)$$

In the atmosphere, methyl hydroperoxide can be found either in aqueous aerosols due to its high solubility,[5] or in the gas phase. In the aerosol phase, it can be washed out from the atmosphere by physical removal processes, i.e. wet and dry deposition. In the gas phase, its most important chemical removal pathways are photolysis and $^{\bullet}OH$-initiated oxidation. These processes are known to play an important role in the redistribution of $HO_x^{\bullet}$ radicals in the troposphere where the oxidation of CH_4 is dominant.[2, 3] The oxidation of CH_3OOH by $^{\bullet}OH$ is known to proceed via two major pathways,[6, 7] (i) abstraction of the hydroperoxide-H to produce $CH_3OO^{\bullet} + H_2O$ (eq. 4), and (ii) abstraction of an αH-atom from the CH_3 group to yield $^{\bullet}CH_2OOH + H_2O$ (eq. 5).

$$CH_3OOH + {}^{\bullet}OH \rightarrow CH_3OO^{\bullet} + H_2O \quad (4)$$

$$CH_3OOH + {}^{\bullet}OH \rightarrow {}^{\bullet}CH_2OOH + H_2O \rightarrow HCHO + {}^{\bullet}OH + H_2O \quad (5)$$

The $^{\bullet}CH_2OOH$ radical is intrinsically unstable, and dissociates spontaneously into $HCHO + {}^{\bullet}OH$.[7, 8] Thus, H-abstraction from the methyl group results in $HCHO + H_2O$, with regeneration of $^{\bullet}OH$, such

that the contribution of channel (5) is not included when the reaction rate coefficient is measured through the decay of $^{\bullet}OH$. On the other hand, the $CH_3OO^{\bullet}$ from channel (4) reacts at low-NO_x concentrations for a large part with $HO_2^{\bullet}$ to re-generate CH_3OOH by reaction (3) such that the net effect will be a chain termination reaction of $^{\bullet}OH$ with $HO_2^{\bullet}$, resulting in the effective removal of $HO_x^{\bullet}$ radicals:

$$^{\bullet}OH + HO_2^{\bullet} \rightarrow H_2O + O_2 \quad (6)$$

At higher NO levels, $CH_3OO^{\bullet}$ can oxidize NO to form $CH_3O^{\bullet}$ and NO_2 of which the first reacts with O_2 to give $HO_2^{\bullet}$ and HCHO, while NO_2 photolyzes quickly into NO and an O atom that immediately adds to O_2 to yield O_3:

$$CH_3OO^{\bullet} + NO \rightarrow CH_3O^{\bullet} + NO_2 \quad (7)$$

$$CH_3O^{\bullet} + O_2 \rightarrow HCHO + HO_2^{\bullet} \quad (8)$$

$$NO_2 + h\nu \rightarrow NO + O \quad (9)$$

$$O + O_2 + M \rightarrow O_3 + M \quad (10)$$

As a result, different from channel (5), pathway (4) will either lead to termination or redistribution of $HO_x^{\bullet}$ radicals. Therefore, both the total rate coefficient and the branching ratio of the title reaction have an impact on atmospheric chemistry, and have to be known for atmospheric modeling.

The overall thermal rate constant at room temperature was measured by Niki et al.[6] to be 1.0×10^{-11} cm^3 s^{-1}, while a value half this magnitude (5.5×10^{-12} cm^3 s^{-1}) was determined by Vaghjiani and Ravishankara.[7] The partial rate constant k_4 for channel (4) was recently re-measured at 295 K by Blitz et al.[3] to be $(9.0 \pm 0.2) \times 10^{-12}$ cm^3 s^{-1}, which is much higher than the two prior measurements, taking into account the branching ratio k_4/k_5 (see below). In the most

recent study, Wang and Chen,[9] using a relative-rate method, re-determined the overall thermal rate constant at 293 ± 2 K to be (4.0 ± 0.15) × 10^{-12} cm^3 s^{-1}, even lower than that of Vaghjiani and Ravishankara.[7] A possible reason for such large discrepancies in the absolute rate determinations could be the challenge to accurately determine the gas-phase concentration of methyl hydroperoxide.

There are two experimental determinations of the branching ratio k_4/k_5 at room temperature: 1.30 ± 0.26 by Niki et al.[6] and the twice higher value 2.52 ± 0.36 by Vaghjiani and Ravishankara[7]. An averaged value of 1.91 ± 0.31 has been recommended,[10] corresponding to yields of 0.65 $\pm$ 0.11 and of 0.35 $\pm$ 0.11 for channels (4) and (5), respectively. The ratio has been estimated to be nearly independent of temperature in the range of T = 220-430 K.[7, 10]

The title reaction has been theoretically studied previously using QCISD[11] and CCSD(T)/CBS(aT,aQ)[12] calculations based on the DFT-BHandHLYP optimized geometries. The rate coefficients of the two H-abstraction pathways were computed at the high-pressure limit, assuming thermal equilibrium[12] between the initial reactants and pre-reactive complexes (PRC), implying a Boltzmann thermal energy distribution for the van der Waals complexes. For the title reaction mechanism passing through a shallow PRC well as displayed in Figure 1, such an assumption can only be fulfilled at very high pressures, but cannot be justified in the Earth's atmosphere (P $\leq$ 1 atm) and in the laboratory where low pressures are often used. The thermal equilibrium model is always to overestimate thermal rate constants significantly. This matter has been discussed recently.[13-16]

Given the large spread of the experimental rate coefficient and branching ratio values, and in view of the invalid assumption - for atmospheric pressures - made in the earlier theoretical

studies above, the aim of the present work is a high-accuracy theoretical investigation of the title reaction at the best currently feasible ab initio and theoretical kinetics methods for such a reaction. As anticipated above, qualitative consideration of Figure 1 indicates that the title reaction is dependent on pressure; thus, solving a master equation must be carried out to obtain reliable thermal rate coefficients.

To this end, high-accuracy coupled-cluster calculations are brought to bear in this work, giving calculated reaction enthalpies that are validated against benchmark ATcT thermochemical data.[17] Phenomenological rate coefficients are then obtained by solving the *E,J*-resolved master equation. On this basis, we derive high-level theoretical $k(T, P)$ and branching ratio values in the temperature range 200-450 K and the pressure range 0 – 10000 Torr, providing also an analytical expression for $k(T)$ at atmospheric pressures useful for atmospheric modeling. Finally, we also compare our theoretical $k(T)$ with the available experimental data.

THEORETICAL METHODOLOGIES

High-Accuracy Coupled-Cluster Calculations

First, key stationary points for the kinetics treatment relevant to two H-abstraction pathways on the lowest-lying doublet electronic state potential energy surface were fully optimized using frozen-core (fc) CCSD(T)/aug-cc-pVTZ level of theory.[18-20] Harmonic vibrational analyses were then performed at the same level of theory to verify all stationary points located: all positive vibrational frequencies for a minimum and only one imaginary frequency (that is corresponding to the reaction coordinate vibration) for a transition structure. To obtain

anharmonic zero-point vibrational energy (ZPE) corrections, anharmonic force field calculations were performed using the same fc-CCSD(T) method, but with a smaller basis set, aug-cc-pVDZ,[21, 22] to save computational time. Total energies including ZPE contributions were then refined using a composite amHEAT-345(Q) method,[23] which gives an accuracy of about 0.2 kcal mol^{-1} as compared to benchmark ATcT values for the two reaction enthalpies as can be seen in Table 1 and Figure 1. The improved amHEAT is obtained by a slight modification of the original mHEAT protocol,[23] in which the basis sets cc-pVXZ (with X=T,Q, and 5)[21, 22] used in the CCSD(T)[18-20] calculations are, respectively, replaced by aug-cc-pVXZ. As detailed elsewhere, the mHEAT-345(Q) protocol[23] generally comprises a series of high-level (single-point energy) coupled-cluster calculations; it recovers a large part of electron correlation with the perturbative triple excitations (CCSD(T)) method and a smaller part of electron correlation with the fully iterative triple (CCSDT) and non-iterative (perturbative) quadruple (CCSDT(Q)) methods.[23] In addition, other small corrections including diagonal Bohr-Oppenheimer correction (DBOC), scalar relativity, and spin-orbit are also included.[23] As demonstrated in Table 1, the anharmonicity ZPE corrections can be important, and are essential in bringing the calculated energies in agreement with the experiment. It should be noted that for the few other reactions[13, 24-26] to which it has already been applied, the amHEAT-345(Q) protocol gives also reaction energies within 0.2 kcal mol^{-1} of the ATcT benchmark values. All calculations (except for the CCSD(T)/ aug-cc-pVQZ and CCSD(T)/ aug-cc-pV5Z single point energy calculations where we have used the ACES III program suite[27]) were done using the CFOUR quantum chemistry package.[28]

Table 1: Individual contributions (kcal mol^{-1}) of various terms to total relative energies of CH_3O_2 + H_2O, HO + HCHO + H_2O, TS1, and TS2 (calculated at 0 K relative to initial reactants, OH + CH_3OOH) using amHEAT-345(Q) method.

Term	OH + HCHO + H_2O	CH_3O_2 + H_2O	TS1	TS2
δE_{SCF}	−60.013	−25.544	15.629	17.940
$\delta E_{CCSD(T)}$	9.191	−8.100	−14.792	−17.011
δE_{ZPE} [a]	−4.141 (−4.214)	0.737 (0.792)	−1.006 (−0.707)	−0.273 (−0.051)
$\delta E_{T-(T)}$	−0.103	−0.271	−0.719	−0.364
$\delta E_{(Q)-T}$	0.158	−0.077	−0.282	−0.222
δE_{Core}	−0.221	−0.135	−0.013	0.007
δE_{Scalar}	0.050	0.055	0.010	0.009
δE_{DBOC}	−0.007	−0.048	0.085	0.001
$\delta E_{Spin-orbit}$	0.000	0.109	0.109	0.109
amHEAT	−55.09 ± 0.2	−33.27 ± 0.2	−0.98 ± 0.2	0.20 ± 0.2
ATcT [b]	−54.82 ± 0.15	−33.17 ± 0.21		

a) The values in parentheses are obtained using harmonic ZPE contributions calculated at fc-CCSD(T)/aug-cc-pVTZ level of theory.

b) Taken from ATcT TN ver. 1.124r.[17]

Two-Dimensional *E,J*-Resolved Master-Equation Calculations

The title reaction proceeds via formation of energized pre-reaction complexes (PRC) of •OH and CH_3OOH (see Fig. 1), thus it is, in principle, expected to be pressure-dependent. The shallow PRC wells of depth ≤ 4 kcal/mol suggest that the high-pressure limit is attained only well above 10 atm. The *E,J*-resolved master equation for a chemically activated reaction as shown in Fig. 1, which describes a competition of collisional energy transfer processes and unimolecular reactions as a function of time, can be given by:[29-37]

$$\frac{\partial C_i(E_m J_m)}{\partial t} = \int_{E_n=0}^{E_{max}} \sum_{J_n=0}^{J_{max}} P_n((E_m J_m | E_n J_n) \cdot \omega_{LJ} \cdot C_i(E_n J_n) \cdot dE_n - \omega_{LJ} \cdot C_i(E_m J_m) - \{k_{i\rightarrow OH}(E_m J_m) + k_{i\rightarrow Products}(E_m J_m)\} \cdot C_i(E_m J_m) + OST_i(E_m J_m) \quad (11)$$

In eq. 11, J_{max} is the maximum angular momentum; E_{max} is the maximum internal energy; $C_i(E_m,J_m,t)$ represents the (time-dependent) mole fractions of PRC_i in the state (E_m,J_m) and time t; and ω_{LJ} (in s^{-1}) is the Lennard-Jones collisional frequency.[38-40] $k_{i\rightarrow Products}(E_m,J_m)$ (in s^{-1}) is the (E_m,J_m)-resolved microcanonical rate coefficient for the dissociation step of PRC_i to products. $k_{i\rightarrow OH}(E_m,J_m)$ is the microcanonical rate constant for the $PRC_i \rightarrow OH + CH_3OOH$ step, which is calculated using micro-variational TST.[41, 42] $P_i(E_m,J_m|E_n,J_n)$ is the *E,J*-resolved collisional transfer probability distribution function of PRC_i from the state (E_n,J_n) to state (E_m,J_m). OST_i stands for the original source term, and is given by:[43-46]

$$OST_i(E_m,J_m) = F_i(E_m,J_m)\cdot k_{i,\infty}(T)\cdot[OH]\cdot[CH_3OOH], \quad (12)$$

$$F_i(E_m,J_m) = \frac{(2J_m+1)\cdot k_{i\rightarrow OH}(E_m,J_m)\cdot\rho_i(E_m,J_m)\cdot\exp(-E_m/RT)}{\sum_{J_m=0}^{J_{max}}(2J_m+1)\int_{E_i=0}^{E_{max}}k_{i\rightarrow OH}(E_m,J_m)\cdot\rho_i(E_m,J_m)\cdot\exp(-E_m/RT)\cdot dE_m}, \quad (13)$$

$$k_{i,\infty}(T) = \frac{\sigma_i}{h}\times\frac{Q_{tr}^i Q_e^i}{Q_{OH}^{re}\cdot Q_{CH_3OOH}^{re}}\times\sum_{J=0}^{\infty}(2J+1)\int_0^{\infty}Min[G_{rv}^{0i}(E,J)]\times\exp\left(-E/k_BT\right)dE \quad (14)$$

Here i is an index, which equals 1 or 2 for the reaction pathway (4) or (5), respectively. $F_i(E_m,J_m)$ is the *E,J*-resolved initial distribution function for the nascent energized PRC_i and given by eq. 12;[43, 46] and $\rho_i(E_m,J_m)$ is the density of ro-vibrational states for PRC_i. $k_{i,\infty}(T)$ is the *capture rate constant* (see eq. 14) – that can be calculated using micro-variational transition state theory (μVTST)[41, 47-49] – for the barrier-less association step of OH and CH_3OOH leading to PRC_i. h is Planck's constant, k_B is Boltzmann's constant, and $\sigma_1=\sigma_2=1$ is the reaction path degeneracy. *T* is the reaction temperature and *E* is the total internal energy. Q_{OH}^{re} and $Q_{CH_3OOH}^{re}$ are the complete

partition functions for •OH and CH_3OOH, respectively. It should be emphasized that for $OH(X^2\Pi)$ (with a spin-orbit splitting of ≈139 cm^{-1}), there is a strong coupling of the 2D rotation and the electronic motion.[50] Thus, the rotational energy values of the components of doublet states of OH were computed using Hill and Van Vleck's formalism.[50-52] The coupled rotational-electronic partition function of •OH was then obtained by a direct state count. Q_{tr}^{i} is the translational partition function, and Q_{e}^{i} is the electronic partition function of the TS_i.

It is worth mentioning that at the zero-pressure limit, an analytical solution of *E,J*-resolved master equation[34] can be derived, and its expression is the same as that of a two-TS kinetic model.[13, 14] Thus, the analytical solution can be given by

$$k_i(T,P=0) = \frac{\sigma_i}{h} \times \frac{Q_{tr}^{i} Q_{e}^{i}}{Q_{OH}^{re} \cdot Q_{CH_3OOH}^{re}} \times \sum_{J=0}^{\infty} (2J+1) \int_{0}^{\infty} \frac{Min[G_{rv}^{0i}(E,J)] \times G_{rv}^{i}(E,J)}{Min[G_{rv}^{0i}(E,J)] + G_{rv}^{i}(E,J)} \times \exp\left(-E/k_B T\right) dE, \quad (15)$$

And $k_{overall}(T)$ is the sum of the $k_i(T,P=0)$ of the two channels (4) and (5).

For the loose, variational TS0i for the barrier-less association of OH and CH_3OOH leading to formation of PRCi*, microvariational TST theory[41, 42] is used to find the kinetic bottleneck, a minimum of the chemical reaction flux ($Min[G_{rv}^{0i}(E,J)]$) at the given *E* and *J* through the dividing surface, eq. 16a. G_{rv}^{0i} is the sum of ro-vibrational quantum states of the TS0i for the given *E* and *J*, which can be obtained from its (harmonic) vibrational counterpart (G_{v}^{0i}) using the *J*-shifting approximation,[53-55] eq. 16a:

$$Min\left[G_{rv}^{0i}(E,J)\right] = Min\left[\sum_{K=-J}^{K=+J} G_{v}^{0i}(E - E_r(J,K))\right], \text{ for a loose TS} \quad (16a)$$

Tables S1 and S2 list the relative energies and rovibrational parameters of grid points along the variational reaction coordinate for OH + $CH_3OOH \rightarrow$ PRC1* and PRC2*, respectively, used in the minimizations.

For the tight, well-defined TS1 and TS2:

$$G_{rv}^{i}(E,J) = \sum_{K=-J}^{K=+J} G_{v}^{i}(E - E_r(J,K)), \qquad (16b)$$

in which G_v^i is the anharmonic (coupled) vibrational sum of states of TS_i that is calculated using Miller's semiclassical TST (SCTST) theory,[56-60] eq. 16b. Non-separable SCTST theory[56-60] automatically includes fully coupled anharmonic vibrations, variational effects, and multi-dimensional quantum mechanical tunneling in the framework of the second-order vibrational perturbation (VPT2) approach. We have used the Wang-Landau algorithm[61-64] as implemented in the Multiwell software package[52] to compute G_v^i. E_r is the (external) rotational energy level of TS1, assuming a symmetric top,[65] eq. 17:

$$E_r(J,K) = J(J+1)\overline{B} + (A - \overline{B})K^2, \text{ with } \overline{B} = \sqrt{B \cdot C} \text{ and } -J \le K \le +J \qquad (17)$$

For three low harmonic vibrational frequencies that are corresponding to large amplitude motions, two for CH_3OOH and one for TS1 (see the Supplementary Material, SM), we consider these vibrations separately from the remaining motions, and treat them as non-coupled one-dimensional hindered internal rotors (1DHR) using the Multiwell software package.[52] We computed the torsional potentials (Figs. S3-S8) and solved the 1D Schrödinger equation to obtain a full set of eigenvalues of each 1DHR (see the SM).[50-52] For each 1DHR, the direct state count was used to compute the quantum states sums; they are combined with those of the remaining motions to obtain the overall sum of ro-vibrational quantum states.

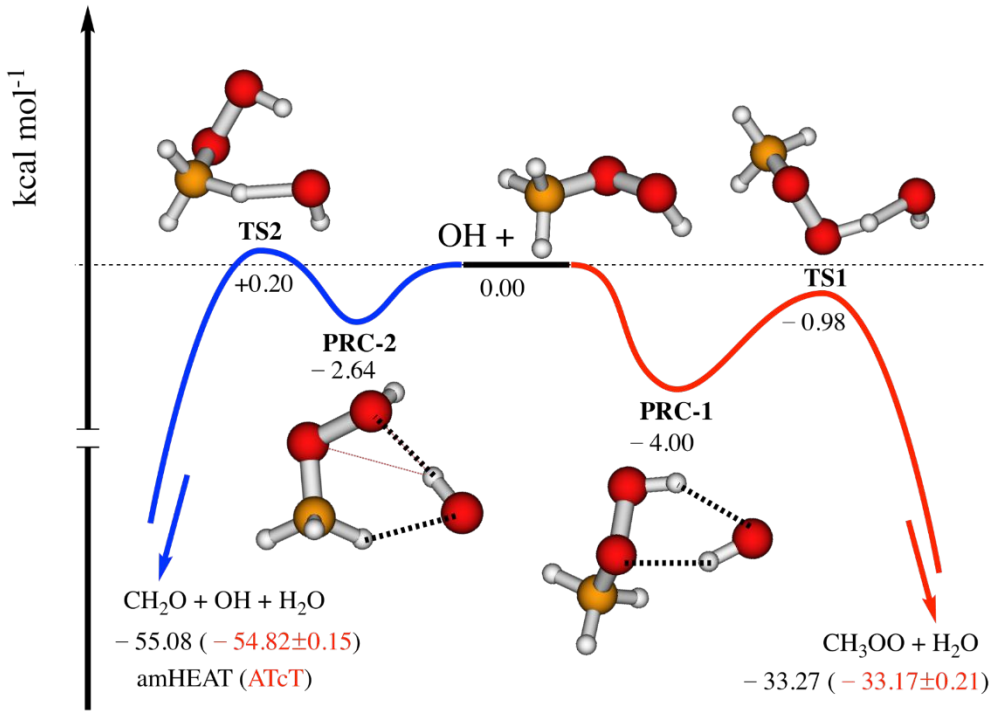

Figure 1: Unscaled potential energy surface for the reaction of OH and CH_3OOH, constructed using the amHEAT-345(Q) method. Benchmark ATcT[17] values (in parentheses) are also included for comparison.

RESULTS and DISCUSSION

Potential Energy Surface and Reaction Mechanism

Figure 1 shows the two feasible H-abstraction pathways for the title reaction. The first proceeds through barrier-less association of $^{\bullet}OH$ with CH_3OOH forming pre-reactive complex **PRC-1**, a five-membered ring stabilized by two hydrogen bonds and located 4.0 kcal mol^{-1} below the initial reactants (Figure 1). Starting from **PRC-1**, two plausible reaction pathways are open: re-dissociation back to the initial reactants via a loose, variational transition state or an intramolecular abstraction of the hydroperoxide-H by the $^{\bullet}OH$ moiety via **TS1,** leading to $CH_3OO^{\bullet}$

+ H_2O. This latter step faces a barrier of 3.0 kcal mol^{-1}. **TS1** is submerged, lying 1.0 kcal mol^{-1} lower in energy than the free reactants in accord with the experimental negative Arrhenius activation energy[7] for this channel. It should be mentioned that there is a higher-lying rotamer of **TS1** that is not shown in Fig. 1, and similar for **TS2**; in the SM these are designated as TS1a and TS2a, respectively. Proper treatment of the hindered internal rotations (1DHR) involved, see below, takes both configurational isomers into account for each case.

Analogously, the second pathway (towards the left in Figure 1) is association without energy barrier leading to **PRC-2**, a six-membered cyclic complex with an even smaller binding energy of −2.64 kcal mol^{-1} in which H-abstraction from the methyl group by the $^{\bullet}OH$ moiety gives rise to a van der Waals complex of $^{\bullet}CH_2OOH$ and H_2O (see Fig. S1 in the SM). This step needs to surmount **TS2** presenting a barrier height of 2.8 kcal mol^{-1}. Note that the energy of **TS2** is *ca.* +0.2 kcal/mol relative to the reactants, and *ca.* 1.2 kcal/mol above that of **TS1** making the second pathway energetically less favored than the first one. The van der Waals complex of $^{\bullet}CH_2OOH$ and H_2O on the product side dissociates spontaneously into HCHO + $^{\bullet}OH$ + H_2O without barrier (see Fig. S1). Our previous calculations[8] revealed that the $^{\bullet}CH_2OOH$ radical is not a local minimum, and is therefore intrinsically unstable, dissociating into HCHO and hydroxyl radical, in accordance with the non-observation of $^{\bullet}CH_2OOH$ in experiments.[7]

It may be noted that for the title reaction, with the lowest TS1 submerged for only 1 kcal mol^{-1}, the first term in the denominator of the integrand in eq. 15 is an order of magnitude larger than the second term for most of the effective energy range, meaning that PRC redissociation far outruns the reaction to products, such that the PRC are in microcanonical quasi-equilibrium with the reactants. As a result, the possible imperfections of the μVTST approach for PRC

redissociation (eq. 15) are of little consequence for the title reaction. The non-separable SCTST theory inherently includes all possible corrections including variational effects in the framework of the second-order vibrational perturbation (VPT2) approach used in this work. In any case, as the tight TS1 and TS2 for H-shifts are well-defined with sharp energy maxima (imaginary frequencies around 1500 cm^{-1}), variational effects should be negligible for the product formation steps, at least at the fairly low temperatures of interest (200-450 K).

Reaction Rate Coefficients and Product Yields

The master equation calculations (see Fig. S2 in the SM) display falloff curves of the title reaction as functions of temperature (200 – 450 K) and pressure (1 – 10000 Torr). Fig. S2 shows that the calculated rate coefficients decrease when temperature increases, while they increase with pressure, but the high-pressure limit is reached only at pressures far above 10000 Torr, as expected. Therefore, these findings are fully consistent with experimental observations.[7] In the range 0 – 10000 Torr considered in this work, the reaction is only slightly dependent on pressure and closely follows the zero-pressure limit under atmospheric conditions ($P \leq 760$ Torr). The rationalization is the very fast redissociation of the large majority of the weakly bound energized PRCs, much faster than the collision frequency, up to *ca.* 10000 Torr. Fig. S3 in the SM shows the high-pressure limit (HPL) rate coefficient (i.e. '*one-TS model*') far exceeding the low-pressure limit at lower temperatures. Because of these reasons without loss of generality, the following results will be reported for the zero-pressure limit.

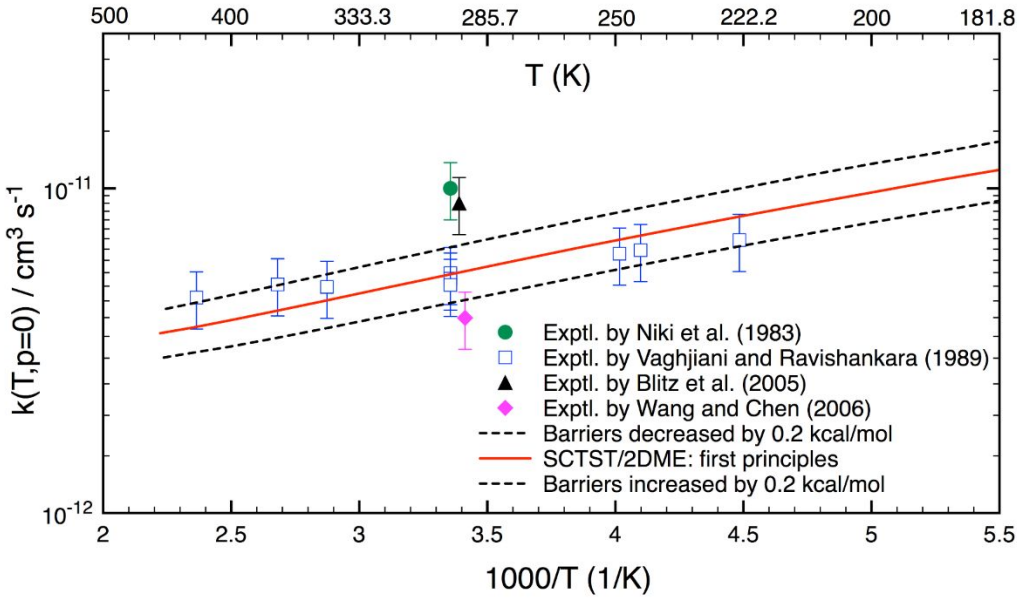

Figure 2: Calculated overall thermal rate constants at the zero-pressure limit as a function of temperature. Dashed lines show the confidence limits for the calculated rate coefficient. Experimental data are also included for comparison; the result of Blitz et al.[3] is k_4, for channel 4 only (see text).

The low-pressure limit $k(T)$ given by eq. (15) were computed as a two-layer function of total energy and total angular momentum using E_{max} = 30,000 cm^{-1}, J_{max} = 200, ΔE = 10 cm^{-1}, and ΔJ = 5. These parameters were selected to ensure that the calculated results converge to within 1% for the temperature range of 180-450 K. The calculated $k(T)$ values are shown in Figure 2, in which all available experimental data are also included for the purpose of comparison. The confidence region *of* $k(T)$ is indicated by the dashed lines, adopting an error on the energy

barriers of +/– 0.2 kcal mol^{-1} (see Table 1). Inspection of Figure 2 shows that the calculated $k(T)$ from first principles only (without any empirical parameters) show a negative temperature dependence, and agree very well, within ~15%, with the experimental results of Vaghjiani and Ravishankara[7] for the whole temperature range (T = 200-450 K). Our results can be fitted to a modified Arrhenius expression of $k(T) = 5.0 \times 10^{-12} \times T^{-0.152} \times \exp\left(\frac{287}{T}\right), in\ cm^3 \cdot s^{-1}$, useful for atmospheric modeling. The value at 298 K is 5.5 × 10^{-12} cm^3 s^{-1}. To the best of our knowledge, this is the only first-principles theoretical work that brings to bear *E,J* resolved microcanonical rate coefficients, resulting in a quantitative agreement with the data of ref. 7. On the other hand, we slightly overestimate the rate constant measured by Wang and Chen,[9] while we underestimate the results of Niki et al.[6] and Blitz et al.[3] by a factor of *ca.* 2.

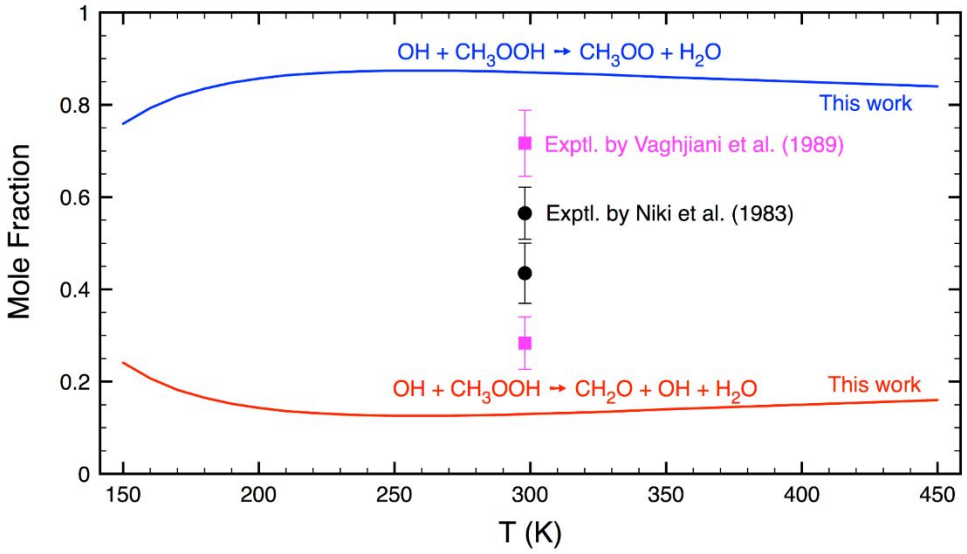

Figure 3: Calculated product branching fractions γ as a function of temperature. Experimental data are also included for comparison.

Our results show that reaction channel (4) to $CH_3OO^{\bullet}$ + H_2O is the principal pathway. A comparison of product branching fractions γ between theory and experiment for the two distinct H-abstraction pathways is shown in Figure 3. As seen there, our theoretical results are higher than the experimental data for formation of $CH_3OO^{\bullet}$ + H_2O, and lower for HCHO + OH + H_2O. In addition, the calculated results depend slightly on temperature in a range of 180-450 K, consistent with the findings in the experimental work of Vaghjiani and Ravishankara.[7] The current study suggests $\gamma = 0.8 \pm 0.1$ for $CH_3OO^{\bullet}$ + H_2O and $\gamma = 0.2 \pm 0.1$ for HCHO + OH + H_2O.

CONCLUSIONS and ATMOSPHERIC IMPLICATIONS

In the present work, the overall thermal rate coefficient and the branching fractions of the title reaction were derived using high-accuracy *ab initio* and advanced theoretical kinetics methods, involving *E,J* resolved microcanonical rate constants. A master equation analysis reveals that the reaction rate constant depends on pressure, although the dependence is only moderate up to 10000 Torr and $k(T)$ is at the low-pressure limit in atmospheric conditions:

$$k(T) = 5.0 \times 10^{-12} \times T^{-0.152} \times \exp\left(\frac{287}{T}\right) cm^3 \cdot s^{-1}, \text{ at T = 200 – 450 K} \quad (18)$$

which reproduces the experimental results of Vaghjiani and Ravishankara,[7] within ~15%, but differs considerably from the other experimental determinations – all at room temperature.

In accord with previous experimental and theoretical studies the title reaction is found to proceed via two channels (4) and (5), which, through their subsequent reactions, have differing impacts on atmospheric chemistry as outlined in the Introduction:

$^{\bullet}OH + CH_3OOH \rightarrow CH_3OO^{\bullet} + H_2O$, $\Delta H_r = -33.2$ kcal mol^{-1}, $\gamma = 0.8 \pm 0.1$ (4)

$^{\bullet}OH + CH_3OOH \rightarrow HCHO + {}^{\bullet}OH + H_2O$, $\Delta H_r = -54.8$ kcal mol^{-1}, $\gamma = 0.2 \pm 0.1$ (5)

The branching fractions γ obtained in this work indicate channel (4) as the major if not dominant pathway. Therefore, it can be stated that at very low NO concentrations the title reaction acts mainly as an $HO_x^\bullet$ sink by the sequence (4) and (3), whereas at higher NO levels it results in $^\bullet OH$ to $HO_2^\bullet$ conversion by the subsequent $CH_3OO^\bullet + NO$ and $CH_3O^\bullet + O_2$ reactions (7) and (8). It can be added that the product $CH_3OO^\bullet$ of channel (4) has recently been shown to react very fast with $^\bullet OH$ to yield largely $CH_3O^\bullet + HO_2^\bullet$, [66-68] which implies overall conversion of 2 $^\bullet OH$ to 2 $HO_2^\bullet$.

In the minor reaction channel (5) the $^\bullet OH$ reactant is regenerated while HCHO is produced. The fate of formaldehyde, resulting also from channel (4) at higher NO levels, is well established.[10, 69] It mainly photolyzes into either $H^\bullet CO + H^\bullet$ or $CO + H_2$, while a smaller fraction reacts with $^\bullet OH$ to form $H^\bullet CO + H_2O$. The first route constitutes a chain-initiation process, the second is neutral with regard to $HO_x^\bullet$ radical chain carriers, while the third converts $^\bullet OH$ to $HO_2^\bullet$. Therefore, the minor pathway (5) is on the whole a net source of $HO_x^\bullet$ radicals through the photolysis of formaldehyde.

On the other hand, the photolysis of CH_3OOH, with rate of (1.1-1.3) × 10^{-6} s^{-1},[70, 71] i.e. a few times slower than the $^\bullet OH$-initiated oxidation at [$^\bullet OH$] = 1.0 × 10^6 cm^{-3}, mainly generates $HO_x^\bullet$ radicals. Since also the production of CH_3OOH from CH_4 by reactions (1a) to (3) acts a $HO_x^\bullet$ sink, it can therefore be concluded that CH_3OOH chemistry is indeed an important redistribution process for $HO_x^\bullet$ radicals in the atmosphere.

Supplementary Material

Optimized geometries, ro-vibrational parameters, anharmonic constants, the calculated rate coefficients, and additional figures and tables are provided in the Supplementary Material.

Acknowledgments

We would like to thank Prof. John F. Stanton for his support and helpful comments to improve the quality of this work. TLN and AP wish to thank the Department of Chemistry, the University of Florida for financial support. This work was supported by the U.S. Department of Energy, Office of Basic Energy Sciences under Award DE-SC0018164. We are grateful to two anonymous reviewers for the useful comments which have led to some significant improvements in the paper.

Data Available

The data that support the findings of this study are available within the article and its supplementary material. Detailed theoretical data that support the findings of this study are available from the corresponding author upon reasonable request.

Authors Contributions

TLN and JP conceived the presented ideas. TLN and AP performed the computations. All authors discussed the results, wrote the manuscript, and contributed to the final manuscript.

Conflicts of Interest: None

References

1. R. Sommariva, A. L. Haggerstone, L. J. Carpenter, N. Carslaw, D. J. Creasey, D. E. Heard, J. D. Lee, A. C. Lewis, M. J. Pilling and J. Zador, *Atmos Chem Phys*, 2004, **4**, 839-856.
2. M. H. Lee, B. G. Heikes and D. W. O'Sullivan, *Atmos Environ*, 2000, **34**, 3475-3494.
3. M. A. Blitz, D. E. Heard and M. J. Pilling, *J Photoch Photobio A*, 2005, **176**, 107-113.
4. G. S. Tyndall, R. A. Cox, C. Granier, R. Lesclaux, G. K. Moortgat, M. J. Pilling, A. R. Ravishankara and T. J. Wallington, *J Geophys Res-Atmos*, 2001, **106**, 12157-12182.
5. D. W. OSullivan, M. Y. Lee, B. C. Noone and B. G. Heikes, *J Phys Chem*, 1996, **100**, 3241-3247.
6. H. Niki, P. D. Maker, C. M. Savage and L. P. Breitenbach, *J Phys Chem*, 1983, **87**, 2190-2193.
7. G. L. Vaghjiani and A. R. Ravishankara, *J Phys Chem*, 1989, **93**, 1948-1959.
8. L. Vereecken, T. L. Nguyen, I. Hermans and J. Peeters, *Chem Phys Lett*, 2004, **393**, 432-436.
9. C. X. Wang and Z. M. Chen, *Prog Nat Sci-Mater*, 2006, **16**, 1141-1149.
10. R. Atkinson, D. L. Baulch, R. A. Cox, J. N. Crowley, R. F. Hampson, R. G. Hynes, M. E. Jenkin, M. J. Rossi and J. Troe, *Atmos Chem Phys*, 2006, **6**, 3625-4055.
11. J. Luo, X. J. Jia, Y. Gao, G. C. Song, Y. B. Yu, R. S. Wang and X. M. Pan, *J Comput Chem*, 2011, **32**, 987-997.
12. J. M. Anglada, R. Crehuet, M. Martins-Costa, J. S. Francisco and M. Ruiz-Lopez, *Phys Chem Chem Phys*, 2017, **19**, 12331-12342.
13. T. L. Nguyen and J. Peeters, *Phys Chem Chem Phys*, 2021, **23**, 16142-16149.
14. T. L. Nguyen and J. F. Stanton, *J Phys Chem A*, 2013, **117**, 2678-2686.
15. D. D. Y. Zhou, K. L. Han, P. Y. Zhang, L. B. Harding, M. J. Davis and R. T. Skodje, *J Phys Chem A*, 2012, **116**, 2089-2100.
16. S. J. Klippenstein, R. Sivaramakrishnan, U. Burke, K. P. Somers, H. J. Curran, L. Cai, H. Pitsch, M. Pelucchi, T. Faravelli and P. Glarborg, *Combust Flame*, 2021, DOI: https://doi.org/10.1016/j.combustflame.2021.111975.
17. B. Ruscic and D. H. Bross, Active Thermochemical Tables (ATcT) values based on ver. 1.122x of the Thermochemical Network (2022), available at ATcT.anl.gov).
18. K. Raghavachari, G. W. Trucks, J. A. Pople and M. Headgordon, *Chem Phys Lett*, 1989, **157**, 479-483.
19. R. J. Bartlett, J. D. Watts, S. A. Kucharski and J. Noga, *Chem Phys Lett*, 1990, **165**, 513-522.
20. J. F. Stanton, *Chem Phys Lett*, 1997, **281**, 130-134.
21. T. H. Dunning, *J Chem Phys*, 1989, **90**, 1007-1023.
22. K. A. Peterson, D. E. Woon and T. H. Dunning, *J Chem Phys*, 1994, **100**, 7410-7415.
23. J. H. Thorpe, C. A. Lopez, T. L. Nguyen, J. H. Baraban, D. H. Bross, B. Ruscic and J. F. Stanton, *J Chem Phys*, 2019, **150**.
24. J. R. Barker, J. F. Stanton and T. L. Nguyen, *Int J Chem Kinet*, 2020, **52**, 1022-1045.
25. T. L. Nguyen and J. F. Stanton, *J Chem Phys*, 2017, **147**, 15204-15207.
26. T. L. Nguyen and A. Perera, *J Phys Chem A*, 2022, **126**, 1966-1972.
27. V. Lotrich, M. Ponton, A. Perera, D. Bokhan, T. J. Watson, T. Kus, A. Yau, N. Jindal, E. Deumens, B. A. Sanders, and R. J. Bartlett, ACES III Program System, Quantum Theory Project, The University of Florida, Gainesville, Florida. 2021.
28. D. A. Matthews, L. Cheng, M. E. Harding, F. Lipparini, S. Stopkowicz, T. C. Jagau, P. G. Szalay, J. Gauss and J. F. Stanton, *J Chem Phys*, 2020, **152**, 214108-214135.
29. S. J. Jeffery, K. E. Gates and S. C. Smith, *J. Phys. Chem.*, 1996, **100**, 7090-7096.
30. S. H. Robertson, M. J. Pilling and N. J. B. Green, *Mol Phys*, 1996, **89**, 1531-1551.
31. J. A. Miller, S. J. Klippenstein and C. Raffy, *J. Phys. Chem.*, 2002, **106**, 4904-4913.
32. A. W. Jasper, K. M. Pelzer, J. A. Miller, E. Kamarchik, L. B. Harding and S. J. Klippenstein, *Science*, 2014, **346**, 1212-1215.
33. P. K. Venkatesh, A. M. Dean, M. H. Cohen and R. W. Carr, *J. Chem. Phys.*, 1999, **111**, 8313-8329.
34. T. L. Nguyen and J. F. Stanton, *J Phys Chem A*, 2020, **124**, 2907-2918.
35. T. L. Nguyen and J. F. Stanton, *J Phys Chem A*, 2015, **119**, 7627-7636.
36. T. L. Nguyen, H. Lee, D. A. Matthews, M. C. McCarthy and J. F. Stanton, *J Phys Chem A*, 2015, **119**, 5524-5533.

37. T. L. Nguyen and J. F. Stanton, *J Phys Chem A*, 2018, **122**, 7757-7767.
38. J. Troe, *J Chem Phys*, 1977, **66**, 4745-4757.
39. R. C. Reid, J. M. Prausnitz and T. K. Sherwood, *The Properties of Gases and Liquids*; McGraw-Hill: New York, 1977.
40. P. D. Neufeld, R. A. Aziz and A. R. Janzen, *J Chem Phys*, 1972, **57**, 1100-1102.
41. W. L. Hase, *Accounts Chem Res*, 1983, **16**, 258-264.
42. D. G. Truhlar and B. C. Garrett, *Annu Rev Phys Chem*, 1984, **35**, 159-189.
43. K. A. Holbrook, M. J. Pilling, S. H. Robertson and P. J. Robinson, *Unimolecular reactions*, Wiley, Chichester ; New York, 2nd edn., 1996.
44. R. G. Gilbert and S. C. Smith, *Theory of unimolecular and recombination reactions*, Blackwell Scientific Publications; Publishers' Business Services distributor, Oxford ; Boston Brookline Village, Mass., 1990.
45. W. Forst, *J Chem Phys*, 1968, **48**, 3665-&.
46. W. Forst, *Unimolecular reactions : a concise introduction*, Cambridge University Press, Cambridge, U.K. ; New York, 2003.
47. H. Eyring, *J Chem Phys*, 1935, **3**, 107-115.
48. M. G. Evans and M. Polanyi, *T Faraday Soc*, 1935, **31**, 0875-0893.
49. D. G. Truhlar, B. C. Garrett and S. J. Klippenstein, *J Phys Chem-Us*, 1996, **100**, 12771-12800.
50. T. L. Nguyen, B. Ruscic and J. F. Stanton, *J Chem Phys*, 2019, **150**, No. 084105.
51. E. Hill and J. H. Van Vleck, *Phys Rev*, 1928, **32**, 0250-0272.
52. J. R. Barker, T. L. Nguyen, J. F. Stanton, C. Aieta, M. Ceotto, F. Gabas, T. J. D. Kumar, C. G. L. Li, L. L. Lohr, A. Maranzana, N. F. Ortiz, J. M. Preses, J. M. Simmie, J. A. Sonk and P. J. Stimac. MULTIWELL Program Suite, Climate and Space Sciences and Engineering; University of Michigan: Ann Arbor, MI, Jan. 2022.
53. W. H. Miller, *J Am Chem Soc*, 1979, **101**, 6810-6814.
54. J. M. Bowman, *J Phys Chem*, 1991, **95**, 4960-4968.
55. N. Balakrishnan, *J Chem Phys*, 2003, **119**, 195-199.
56. W. H. Miller, *Faraday Discuss*, 1977, **62**, 40-46.
57. W. H. Miller, R. Hernandez, N. C. Handy, D. Jayatilaka and A. Willetts, *Chem Phys Lett*, 1990, **172**, 62-68.
58. R. Hernandez and W. H. Miller, *Chem Phys Lett*, 1993, **214**, 129-136.
59. T. L. Nguyen, J. F. Stanton and J. R. Barker, *Chem Phys Lett*, 2010, **499**, 9-15.
60. T. L. Nguyen, J. F. Stanton and J. R. Barker, *J Phys Chem A*, 2011, **115**, 5118-5126.
61. F. G. Wang and D. P. Landau, *Phys Rev Lett*, 2001, **86**, 2050-2053.
62. F. G. Wang and D. P. Landau, *Phys Rev E*, 2001, **64**, No. 056101.
63. M. Basire, P. Parneix and F. Calvo, *J Chem Phys*, 2008, **129**, No. 081101.
64. T. L. Nguyen and J. R. Barker, *J Phys Chem A*, 2010, **114**, 3718-3730.
65. T. Baer and W. L. Hase, *Unimolecular reaction dynamics : theory and experiments*, Oxford University Press, New York, 1996.
66. J. F. Muller, Z. Liu, V. S. Nguyen, T. Stavrakou, J. N. Harvey and J. Peeters, *Nature Communications*, 2016, **7**, 13213.
67. E. Assaf, L. Sheps, L. Whalley, D. Heard, A. Tomas, C. Schoemaecker and C. Fittschen, *Environmental Science & Technology*, 2017, **51**, 2170-2177.
68. R. L. Caravan, M. A. H. Khan, J. Zador, L. Sheps, I. O. Antonov, B. Rotavera, K. Ramasesha, K. Au, M. W. Chen, D. Rosch, D. L. Osborn, C. Fittschen, C. Schoemaecker, M. Duncianu, A. Grira, S. Dusanter, A. Tomas, C. J. Percival, D. E. Shallcross and C. A. Taatjes, *Nature Communications*, 2018, **9**, 4343.
69. R. Atkinson, *J. Phys. Chem. Ref. Data*, 1997, **26**, 215-290.
70. G. L. Vaghjiani and A. R. Ravishankara, *J Geophys Res-Atmos*, 1989, **94**, 3487-3492.
71. C. M. Roehl, Z. Marka, J. L. Fry and P. O. Wennberg, *Atmos Chem Phys*, 2007, **7**, 713-720.